Two-step optogalvanic spectroscopy of neutral barium: Observations and interpretation of the even levels below the 6s ionization limit with $J=1$, 3, 4, and 5

P. Camus, M. Dieulin, and A. El Himdy
Laboratoire Aimé Cotton, C.N.R.S. II, Bâtiment 505, 91405 Orsay, France
(Received 2 July 1981)

Even-parity levels of neutral barium located in the vicinity of the first ionization limit 6*s* have been investigated by using a two-step pulsed-laser excitation with optogalvanic detection. From the metastable states $5d\,6s$ populated by a dc discharge in a heat-pipe vapor, we reach the $6snl$ even-Rydberg series with J equal to 0 to 5 and all the levels of the $5d\,6d$ and $5d\,7d$ configurations via the intermediate $5d\,6p$ levels. The $6sns\ ^3S_1$ ($13 \leq n \leq 47$) and $6snd\ ^3D_1$ ($12 \leq n \leq 38$) series are observed for the first time with five perturbers assigned to $5d\,8s\ ^3D_1$, $5d\,7d\ ^3D_1$, $^3S_1$, $^1P_1$, and $^3P_1$. The $6snd\ ^3D_3$ ($11 \leq n \leq 24$) series is perturbed by five levels $5d\,8s\ ^3D_3$, $5d\,7d\ ^3G_3$, $^1F_3$, $^3D_3$, and $^3F_3$. The fine structure of the $6dng\ ^{1,3}G$ series is partially resolved in the vicinity of the perturbing $5d\,7d$ $J=3$, 4, and 5 levels. Semiempirical calculations using Racah's method have allowed us to understand the observed energies of the levels belonging to $5d\,6d$ and $5d\,7d$ configurations and to remove the ambiguity which was subsisting in the literature for the energy position of the $6p^2\ ^1S_0$ level.

I. INTRODUCTION

In this paper, we describe a two-step excitation process associated with an optogalvanic detection of the resonances to study the highly excited even levels of barium around the first ionization limit 6*s*. Preliminary results have already been published.[1]

The basic concept of optogalvanic effect, first observed by Penning[2] irradiating a neon discharge lamp with the light emitted from a second neon lamp and recently developed when tunable dye laser became available,[3,4] is that atoms selectively excited by resonant laser irradiation to higher-energy levels ionized more easily in a glow discharge or flames. The enhancement of the ionization rate causes an increasing charge density in the plasma, which is then measured by a decrease of the applied voltage needed to maintain the discharge. Moreover, optogalvanic spectroscopy (OG) is more precisely labeled laser enhanced ionization spectroscopy (LEI) by flame's spectroscopists.

Until now observations of highly excited levels (Rydberg levels) in multiphoton or multistep laser spectroscopy were generally limited to processes starting from the ground level $6s^2\ J=0$ of neutral barium and consequently restricted to the J values obeying the selection rules involved by the excitation used. Previous measurements of the even $J=0$ and $J=2$ levels of Ba I below the ionization limit 6*s* have been made using photographic absorption spectroscopy from excited levels populated with a dye laser[5,6] and extensive new data on the $6sns\ ^1S_0$ and $6snd\ ^{1,3}D_2$ Rydberg series have been obtained using two-photon absorption spectroscopy with a nitrogen-pumped dye laser and a space-charge limited thermoionic diode as an ion detector.[7] All these observations starting from the ground level $J=0$, were limited to upper levels with $J=0$, 1, or 2 in the two-step experiment and $J=0$ or 2 in the two-photon selective excitation. Bound even-parity $J=0$ (Ref. 7) and $J=2$ (Refs. 8 and 9) spectra, successfully interpreted by means of the multichannel quantum-defect theory (MQDT) have shown important interacting perturbers of the $6sns\ ^1S_0$ and $6snd\ ^{1,3}D_2$ series belonging to $5dns$ ($n=7$, 8), $5dnd$ ($n=6,7$), and $6p^2$ configurations.

In order to extend the J-level knowledge of each even $6snl$ series and their perturbers pertaining to $5d\,8s$ (two $J=1$ and 3 unknown levels) and $5d\,7d$ (15 unknown levels with J values from 0 to 5) configurations, processes using more than two photons or two steps are needed. But the experimental arrangement becomes more complex and particularly the analysis of the obtained records is not so obvious owing to the increased number of multistep ways that occurs simultaneously in a few Torr vapor pressure of barium.

Under these conditions, further investigations

are needed with optical transitions starting from excited levels populated by a nonoptical process and we used a glow discharge in a heat-pipe cell[10] which has provided, a few years ago, an easy way to increase the population density of the low-even $5d\,6s\ ^1D_2$ and $5d\,6s\ ^3D_{1,2,3}$ metastable levels. Starting from one of these low-excited levels, we carry out the measurements of the impedance changes of the discharge, when a two-step resonant laser excitation is realized leading to an even upper level via an odd intermediate $5d\,6p$ level. With this compact technique which provides at the same time, two different functions, electric discharge collisional population of the low $5d\,6s$ metastable levels and ionic detection of the optical resonant transitions in the plasma, we have been able to observe a large number of bound highly excited even levels with J values ranging from 0 to 5.

We completed our previous work on $J=0$ and $J=2$ levels using two-photon absorption experiment by measuring the $5d\,7d\ ^1S_0$ and $5d\,7d\ ^3D_2$ and $^3P_2$ missing levels. Moreover we observed the $6sns\ ^3S_1$ $(13 \leq n \leq 47)$ and $6snd\ ^3D_1$ $(12 \leq n \leq 38)$ series with five perturbers, the $6snd\ ^3D_3$ $(11 \leq n \leq 24)$ series with five perturbers, and the $6sng\ ^{1,3}G$ $(8 \leq n \leq 39)$ unresolved series with four perturbers. The complete structure of the $5d\,7d$ doubly excited configuration (18 states) is observed and interpreted by means of the Slater-Condon parametric study using Racah's method. Assignments of the $5d\,7d$ levels in LS- and jj-coupling schemes are compared to those of the $5d\,6d$ configuration.

Before presenting experimental results concerning the $J=1$, 3, 4, and 5 spectra (Sec. III) and the parametric studies of the $5d\,6d$ and $5d\,7d$ configurations (Sec. IV), we give a complementary detailed discussion of the experimental method (Sec. II) previously described.[1]

II. EXPERIMENTAL METHOD

Two-step excitations take place in a glow-discharge of Ba vapor maintained in a heat-pipe cell. The experimental arrangement is shown in Fig. 1.

A Molectron uv-1000 nitrogen-pulsed laser is used to pump two similar dye lasers with a 15-Hz repetition rate. The pulse duration is about 10 ns and the laser linewidth is 0.3 cm^{-1}. The two dye laser beams are counterpropagating axially through the discharge tube for convenience and not for Doppler width (~ 0.06 cm^{-1}) elimination by taking in account the instrumental linewidth (~ 0.3 cm^{-1}).

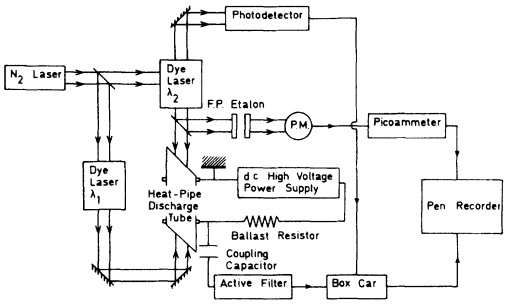

FIG. 1. Experimental setup for two-step optogalvanic spectroscopy.

The discharge tube[10,1] shown in Fig. 2 operates at 20 mA-400 V for a 2.3—2.7 Torrs vapor pressure of barium corresponding to an electric furnace temperature between 905 and 935 °C. The ac component of the potential across the tube is displayed on an oscilloscope and recorded on an electronic device through a 6 800 pF blocking capacitor and a bandpass active filter (110-kHz central frequency, 90-kHz bandwidth, and a gain about 17 for the optogalvanic signals). Residual noise of the discharge after the filter is about 3 mV when the cell operates at the required conditions to reach the equilibrium between the liquid and the gaseous phases of the vaporized element. Below this point, the cell works as a conventional absorption cell with a mixture of He and Ba excited atoms and then the electric noise is considerably increased by a factor 100 or more.

There is no doubt that the stability of the discharge in the plasma depends strongly on the density of charges and is greatly enhanced when the homogeneous vapor density of atoms is ruled by the heat-pipe working conditions. When interacting with the pulsed-dye laser tuned to an atomic transition, the perturbed discharge returns to its previous steady permanent regime with different shapes of transient optogalvanic signals. Similar signals have been studied for argon and neon carrier gases in uranium hollow cathode lamp[11] and are presented in the previous paper.[1]

The first dye laser is easily tuned to the first-step transition between one of the $5d\,6s$ metastable levels and a chosen intermediate $5d\,6p$ level by looking at the superposed spectra emitted by the glow discharge and the laser line through a low resolving power (± 4 Å) Jobin-Yvon grating spectroscope. Exact tuning frequency is then achieved by optimizing the optogalvanic signal displayed on the oscilloscope. For the first step allowed transi-

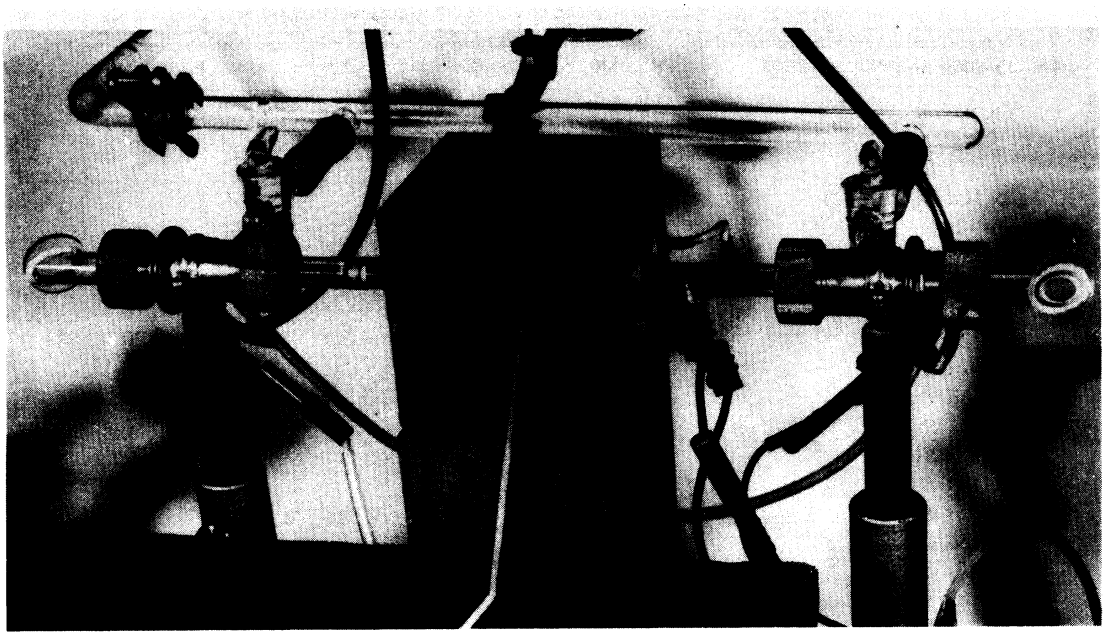

FIG. 2. Discharge heat-pipe cell for optogalvanic detection.

tions between $5d\,6s$ and $5d\,6p$ levels, the first negative peak amplitude of the signal is around ~ 50 mV. Then, the second dye laser is scanned in order to explore even highly excited levels in the discrete and autoionized region as shown in the Fig. 3. Recorded optogalvanic spectrum is referenced to calibrated transmission maxima of a vacuum-spaced Fabry-Perot interferometer illuminated with a small part of the second-step laser beam which gives a constant frequency interval between two peaks of $1.314\,678 \pm 0.000\,001$ cm^{-1}.

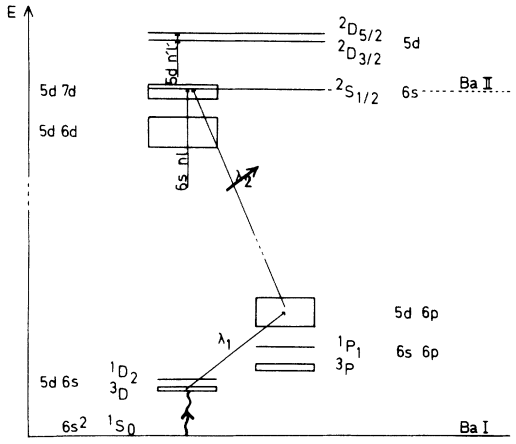

FIG. 3. Schematic barium levels diagram.

Absolute calibration of the two-step optogalvanic spectrum is made by reference to several one-step previously classified lines which present a good signal-to-noise ratio and a symmetrical profile. The energies of the new identified even levels are then calculated by adding the measured wavenumber of the second-step line to the energy of the intermediate $5d\,6p$ level involved in the two-step resonance. The energies of the $5d\,6p$ levels given in Ref. 12 have been accurately redetermined with a ± 0.05 cm^{-1} uncertainty by Verges[13] from new infrared Fourier transform spectra of Ba recorded in the range $1-2.5\ \mu$ at Aimé Cotton. For $J=0$ and $J=2$ levels, averaged values from several optogalvanic spectra have been compared to previous two-photon measurements[7]: maximum observed shift is less than 0.08 cm^{-1}. We estimate the energy uncertainty to be less than ± 0.100 cm^{-1} for the new even levels given in Tables I–IV. No appreciable Stark shifts have been observed except the Stark broadening of the high-lying lines of the $6snl$ series above $n \sim 35$.

TABLE I. Observed even-parity $J=1$ bound levels of Ba I.

Designation	E_{obs} (cm^{-1})	Error (cm^{-1})
$6s\,9d\,^3D_1$	39 140.70[a]	
$\underline{5d\,8s}\,^3D_1$	39 382.78	0.10
$6s\,11s\,^3S_1$	39 624.69[a]	
$6s\,10d\,^3D_1$	39 892.19[a]	
$6s\,12s\,^3S_1$		
$6s\,11d\,^3D_1$	40 407.38	0.10
$6s\,13s\,^3S_1$	40 568.98	0.10
$\underline{5d\,7d}\,^3D_1$	40 684.38	0.10
$6s\,12d\,^3D_1$	40 742.6	0.20
$6s\,14s\,^3S_1$	40 869.7	0.20
$6s\,13d\,^3D_1$	40 982.35	0.05
$\underline{5d\,7d}\,^3S_1$	41 019.54	0.14
$6s\,15s\,^3S_1$	41 082.22	0.05
$6s\,14d\,^3D_1$	41 162.99	0.05
$6s\,16s\,^3S_1$	41 235.82	0.06
$6s\,15d\,^3D_1$	41 299.55	0.05
$6s\,17s\,^3S_1$	41 356.21	0.05
$6s\,16d\,^3D_1$	41 406.49	0.05
$6s\,18s\,^3S_1$	41 451.23	0.07
$6s\,17d\,^3D_1$	41 491.53	0.07
$6s\,19s\,^3S_1$	41 527.12	0.08
$6s\,18d\,^3D_1$	41 558.98	0.05
$\underline{5d\,7d}\,^1P_1$	41 570.34	0.05
$6s\,20s\,^3S_1$	41 592.68	0.05
$6s\,19d\,^3D_1$	41 617.77	0.10
$6s\,21s\,^3S_1$	41 642.76	0.06
$6s\,20d\,^3D_1$	41 664.65	0.08
$6s\,22s\,^3S_1$	41 685.66	0.05
$6s\,21d\,^3D_1$	41 704.17	0.05
$6s\,23s\,^3S_1$	41 721.93	0.05
$6s\,22d\,^3D_1$	41 737.72	0.07
$6s\,24s\,^3S_1$	41 752.78	0.05
$6s\,23d\,^3D_1$	41 766.30	0.06
$6s\,25s\,^3S_1$	41 779.34	0.05
$6s\,24d\,^3D_1$	41 791.08	0.05
$6s\,26s\,^3S_1$	41 802.46	0.10
$6s\,25d\,^3D_1$	41 812.40	0.06
$6s\,27s\,^3S_1$	41 822.32	0.05
$6s\,26d\,^3D_1$	41 831.16	0.12
$6s\,28s\,^3S_1$	41 839.84	0.06
$6s\,27d\,^3D_1$	41 847.75	0.05
$6s\,29s\,^3S_1$	41 855.34	0.05
$6s\,28d\,^3D_1$	41 862.29	0.05
$6s\,30s\,^3S_1$	41 869.04	0.05
$6s\,29d\,^3D_1$	41 875.19	0.05
$6s\,31s\,^3S_1$	41 881.15	0.10
$6s\,30d\,^3D_1$	41 886.70	0.05
$6s\,32s\,^3S_1$	41 892.03	0.10
$6s\,31d\,^3D_1$	41 897.02	0.05
$6s\,33s\,^3S_1$	41 901.82	0.06
$6s\,32d\,^3D_1$	41 906.31	0.05
$6s\,34s\,^3S_1$	41 910.55	0.06
$6s\,33d\,^3D_1$	41 914.55	0.05
$6s\,35s\,^3S_1$	41 918.43	0.07

TABLE I. (*Continued.*)

Designation	E_{obs} (cm^{-1})	Error (cm^{-1})
$6s\,34d\,^3D_1$	41 922.18	0.05
$6s\,36s\,^3S_1$	41 925.44	0.08
$6s\,35d\,^3D_1$	41 928.78	0.05
$\underline{5d\,7d}\,^3P_1$	41 930.88	0.15
$6s\,37s\,^3S_1$	41 933.60	0.17
$6s\,36d\,^3D_1$	41 935.41	0.05
$6s\,38s\,^3S_1$	41 938.79	0.08
$6s\,37d\,^3D_1$	41 940.73	0.25
$6s\,39s\,^3S_1$	41 944.14	0.06
$6s\,38d\,^3D_1$	41 946.13	0.20
$6s\,40s\,^3S_1$	41 949.09	0.05
$6s\,39d\,^3D_1$		
$6s\,41s\,^3S_1$	41 953.61	0.05
$6s\,42s\,^3S_1$	41 957.90	0.05
$6s\,43s\,^3S_1$	41 961.79	0.05
$6s\,44s\,^3S_1$	41 965.43	0.05
$6s\,45s\,^3S_1$	41 968.82	0.06
$6s\,46s\,^3S_1$	41 971.90	0.10
$6s\,47s\,^3S_1$	41 974.85	0.10
$6s\,48s\,^3S_1$		

[a]Reference 12.

TABLE II. Observed even-parity $J=3$ bound levels of Ba I.

Designation	E_{obs} (cm^{-1})	Error (cm^{-1})
$6s\,9d\,^3D_3$	39 185.75[a]	
$6s\,10d\,^3D_3$	39 905.15[a]	
$\underline{5d\,8s}\,^3D_3$	40 146.62	0.06
$6s\,11d\,^3D_3$	40 423.39	0.05
$6s\,9g\,^3G_3$	40 663.93	0.13
$\underline{5d\,7d}\,^3G_3$	40 698.58	0.08
$6s\,12d\,^3D_3$	40 748.18	0.05
$\underline{5d\,7d}\,^1F_3$	40 867.29	0.09
$6s\,13d\,^3D_3$	40 987.20	0.07
$6s\,14d\,^3D_3$	40 164.70	0.05
$6s\,15d\,^3D_3$	41 300.80	0.12
$6s\,13g\,^3G_3$	41 379.94	0.10
$6s\,16d\,^3D_3$	41 405.95	0.10
$\underline{5d\,7d}\,^3D_3$	41 459.36	0.08
$6s\,14g\,^3G_3$	41 470.94	0.10
$6s\,17d\,^3D_3$	41 495.60	0.09
$6s\,18d\,^3D_3$	41 562.55	0.05
$6s\,19d\,^3D_3$	41 618.44	0.19
$6s\,20d\,^3D_3$	41 665.29	0.12
$6s\,21d\,^3D_3$	41 704.46	0.05
$\underline{5d\,7d}\,^3F_3$	41 726.61	0.05
$6s\,19g\,^3G_3$	41 729.46	0.10
$6s\,22d\,^3D_3$	41 739.11	0.17
$6s\,23d\,^3D_3$	41 767.16	0.10
$6s\,24d\,^3D_3$	41 791.72	0.10

[a]Reference 12.

TABLE III. Observed even-parity $J=3$, 4, and 5 bound levels of Ba I.

Designation	E_{obs} (cm^{-1})	Error (cm^{-1})
$6s\,8g\,^{1,3}G$	40 300.01	0.05
$6s\,9g\,^{3}G_3$	40 663.93	0.13
$6s\,9g\,^{1,3}G$	40 665.54	0.05
$\underline{5d\,7d}\,^{3}G_3$	40 698.58	0.08
$\underline{5d\,7d}\,^{1}f_3$	40 867.29	0.09
$6s\,10g\,^{3}G_4$	40 925.39	0.05
$6s\,10g\,^{1,3}G$	40 926.75	0.05
$\underline{5d\,7d}\,^{3}G_4$	40 974.28	0.07
$6s\,11g\,^{1,3}G$	41 119.20	0.10
$6s\,11g\,^{3}G_4$	41 119.97	0.09
$6s\,12g\,^{1,3}G$	41 266.44[a]	0.05
$6s\,13g\,^{3}G_3$	41 379.94[a]	0.10
$6s\,13g\,^{1,3}G$	41 380.34	0.10
$\underline{5d\,7d}\,^{3}D_3$	41 459.37	0.09
$6s\,14g\,^{1,3}G$	41 470.57	0.08
$6s\,14g\,^{3}G_3$	41 470.94	0.05
$6s\,15g\,^{3}G_5$	41 539.67	0.05
$6s\,15g\,^{1,3}G$	41 543.74[a]	0.05
$\underline{5d\,7d}\,^{3}G_5$	41 550.27	0.10
$6s\,16g\,^{1,3}G$	41 603.46	0.10
$6s\,16g\,^{3}G_5$	41 603.87	0.05
$6s\,17g\,^{1,3}G$	41 652.77[a]	0.10
$6s\,17g\,^{3}G_5$	41 653.05	0.05
$6s\,18g\,^{3}G_3$	41 693.89[a]	0.10
$6s\,18g\,^{1,3}G_3$	41 694.31	0.10
$\underline{5d\,7d}\,^{3}F_3$	41 726.61	0.05
$6s\,19g\,^{1,3}G$	41 729.46[a]	0.11
$6s\,20g\,^{1,3}G$	41 759.07	0.05
$6s\,21g\,^{1,3}G$	41 784.79[a]	0.05
$6s\,22g\,^{1,3}G$	41 807.14[a]	0.05
$6s\,23g\,^{1,3}G$	41 826.30[a]	0.05
$6s\,24g\,^{3}G_4$	41 842.22	0.05
$6s\,24g\,^{1,3}G$	41 843.90[a]	0.30
$\underline{5d\,7d}\,^{3}F_4$	41 845.61	0.05
$6s\,25g\,^{1,3}G$	41 858.70[a]	0.10
$6s\,25g\,^{3}G_4$	41 858.89	0.10
$6s\,26g\,^{1,3}G$	41 871.79[a]	0.10
$6s\,26g\,^{3}G_4$	41 872.00	0.05
$6s\,27g\,^{1,3}G$	41 883.82[a]	0.05
$6s\,28g\,^{1,3}G$	41 894.42	0.07
$6s\,29g\,^{1,3}G$	41 903.86[a]	0.06
$6s\,30g\,^{1,3}G$	41 912.54[a]	0.10
$6s\,31g\,^{1,3}G$	41 920.46[a]	0.10
$6s\,32g\,^{1,3}G$	41 927.50[a]	0.10
$6s\,33g\,^{1,3}G$	41 934.00	0.10
$6s\,34g\,^{1,3}G$	41 939.90[a]	0.10
$6s\,35g\,^{1,3}G$	41 945.33[a]	0.10
$6s\,36g\,^{1,3}G$	41 950.22[a]	0.15
$6s\,37g\,^{1,3}G$	41 954.72	0.15
$6s\,38g\,^{1,3}G$	41 958.92[a]	0.15
$6s\,39g\,^{1,3}G$	41 962.71	0.15

[a]Reference 9.

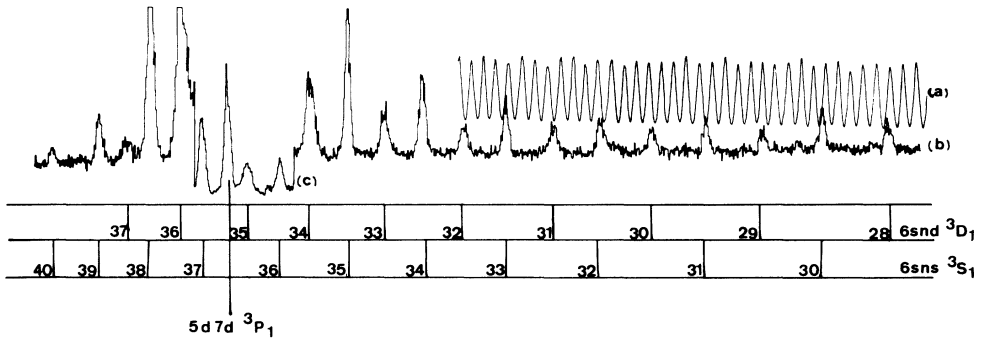

FIG. 4. Two-step optogalvanic spectrum of barium. (a) Fabry-Perot fringes $\Delta\sigma = 1.314\,67(8)$ cm^{-1}; (b) spectrum of Ba with $5d\,6s\ ^3D_1$-$5d\,6p\ ^3P_0^o$: 6019.5 Å for the first-step transition in the vicinity of the $5d\,7d\ ^3P_1$ perturber; (c) the second-step laser is attenuated by 10.

III. RESULTS

The energies of the $J = 1$, 3, 4, and 5 new levels observed from 40 000 cm^{-1} up to the 6*s* ionization limit are given in Tables I–III.

A. $J = 1$ even levels

Sixty-seven new even-parity $J = 1$ levels have been established from two-step laser excitation and optogalvanic detection using successively $5d\,6p\ ^3P_0^o$: 25 642.10 cm^{-1}, $^3P_1^o$: 25 704.08 cm^{-1}, and $^3P_2^o$: 25 956.49 cm^{-1} as intermediate levels and two dyes (Rhodamine B and 640) for the second step. The observed $6sns\ ^3S_1$ and $6snd\ ^3D_1$ series have been extended from $n = 13$ to $n = 47$ and from $n = 12$ to $n = 38$, respectively. In the first approximation, if we suppose pure intermediate $5d\,6p$ states, electric dipolar transitions are not allowed between $5d\,6p$ odd levels and unperturbed high-lying $6sns$ and $6snd$ levels. In the preliminary paper,[1] we can see the picture giving the two-step optogalvanic near the strong $5d\,7d\ ^1D_2$ perturber with the $5d\,6p\ ^3P_2^o$ as intermediate level. Along the series line intensities increase on both sides of the perturber. Oscillator strengths for the second step qualitatively follow the admixture of the $5d_{3/2}nd_{3/2}$ channel given in the MQDT study of the $6snd\ ^{1,3}D_2$ series[8] which is characterized by a large mixing with the $^3D_2$ states below the perturber and with the $^1D_2$ states above. The same mixing effects on $6snl$ series have been observed for many other new $5d\,7d$ perturbers and are useful to identify them unambiguously.

For the $J = 1$ levels, five perturbers with $5d\,8s\ ^3D_1$ (39 382 cm^{-1}) and with $5d\,7d$ levels: $^3D_1$ (40 684 cm^{-1}), $^3S_1$ (41 019 cm^{-1}), $^1P_1$ (41 570 cm^{-1}), and $^3P_1$ (41 930 cm^{-1}). The energy distribution of these levels below the first ionization limit explains the extensive data obtained. Low

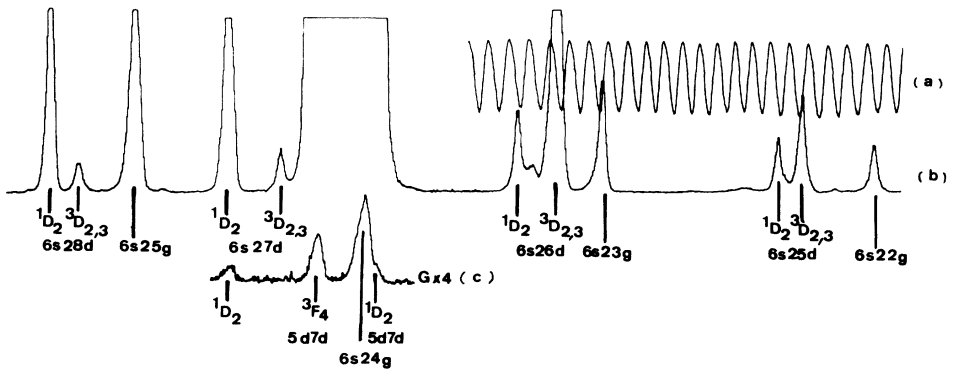

FIG. 5. Two-step optogalvanic spectrum of barium. (a) Fabry-Perot fringes $\Delta\sigma = 1.314\,67(8)$ cm^{-1}; (b) spectrum of Ba with $5d\,6s\ ^3D_2 - 5d\,6p\ ^3F_3^o$: 7280.3 Å for the first-step transition in the vicinity of the $5d\,7d\ ^1D_2$ and $^3F_4$; (c) same spectrum with only the second-step laser.

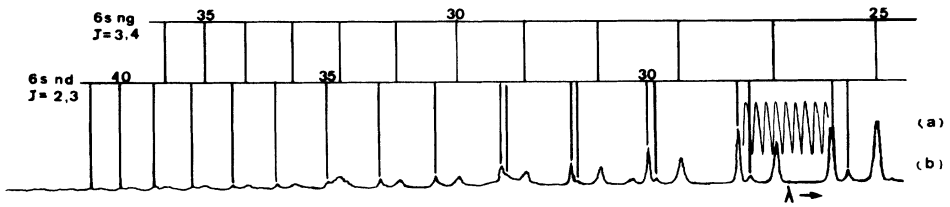

FIG. 6. Two-step optogalvanic spectrum of barium. (a) Fabry-Perot fringes $\Delta\sigma = 1.314\,67(8)$ cm^{-1}; (b) spectrum of Ba with $5d\,6s\ ^3D_2$-$5d\,6p\ ^3F_3^o$: 7280.3 Å for the first-step transition below the 6s ionization limit.

missing levels $6s\,12s\ ^3S_1$ has been unsuccessfully searched at the energy position predicted by a one-channel quantum-defect theory using the $6s\,6p\ ^1P_1^o$ intermediate level.

Above $n = 20$, fine structure of the $6snd\ ^3D$ term is normally unresolved by taking in account the 0.300 cm^{-1} instrumental linewidth (FWHM), and we observed complex line structures with $5d\,6p\ ^3P_1^o$ (two components) and $^3P_2^o$ (three components) intermediate levels. Measurements from simple peak spectrum with $5d\,6p\ ^3P_0^o$ level have been used for the energy determination.

The level at 41 451 cm^{-1} interpreted as $6s\,18s\ ^1S_0$ in Ref. 6 and not confirmed in the $J = 0$ and $J = 2$ two-photon spectra[7] is a real level with $J = 1$ interpreted as $6s\,18s\ ^3S_1$. The $5d\,8s\ ^3D_1$ level has been established at 39 382 cm^{-1} by a strong two-step resonance using the $5d\,6p\ ^3D_2^o$ intermediate level: 24 531.49 cm^{-1}.

Figure 4 shows the optogalvanic spectrum recorded as a function of λ_2 in the vicinity of the $5d\,7d\ ^3P_1$ perturber, using the $5d\,6p\ ^3P_0^o$ intermediate level.

B. $J = 3$ even levels

Twenty-three new $J = 3$ levels have been found by applying J-selection rule from observed two-step laser excitation using $5d\,6p\ ^3P_2^o$, $^3D_3^o$: 24 979.81 cm^{-1}, and $^3F_4^o$: 23 757.03 cm^{-1} intermediate levels and three dyes (Rhodamine B, 640, and 6G) for the second-step laser line. The numbers of the $6snd\ ^3D_3$ series have been observed from $n = 11$ up to $n = 24$ because of configuration mixing with five levels identified to $5d\,8s\ ^3D_3$ (40 146 cm^{-1}) and to $5d\,7d$: $^3G_3$ (40 698 cm^{-1}), $^1F_3$ (40 867 cm^{-1}), ^3D_s (41 459 cm^{-1}), and $^3F_3$ (41 726 cm^{-1}). Energy value of the $6snd\ ^3D_3$ levels are obtained from the analysis of the simple peaks series observed from the $5d\,6p\ ^3F_4^o$ intermediate level. As discussed in the next paragraph fine structure of the $6sng\ ^{1,3}G$ series is only solved for the $J = 3$ $6s\,9g$, $6s\,13g$, $6s\,14g$, and $6s\,19g$ levels lying near the $5d\,7d$ perturbers.

TABLE IV. Observed levels of $5d\,7d$ above the first ionization limit 6s of Ba I.

Designation	E_{obs} (cm^{-1})	Error (cm^{-1})
$5d\,7d\ ^1G_4$	42 041.77	0.2
$5d\,7d\ ^3P_2$	42 118.40	0.2
$5d\,7d\ ^1S_0$	42 370.51	0.4

C. $J = 3$, 4, and 5 even levels belonging to $6sng$ series and $5d\,7d$ perturbing levels

Twenty-three new levels with $J = 3$, 4, and 5 are listed in Table III with identified $6sng$ and $5d\,7d$ $J = 3$, 4, and 5 levels. Due to the expected small value of the spin-orbit coupling for an ng electron, fine structure of the $6sng$ group of four levels is unsolved even for the $6s\,8g$ lowest member observed. The measured energy of the unresolved peak from the $5d\,6p\ ^3F_4^o$ intermediate level is assigned to the $6sng\ ^{1,3}G$ states. Our $6sng\ ^{1,3}G$ energy measurements are in close agreement with $6sng\ ^1G_4$ observations previously obtained by Armstrong *et al.*[9] in a three-photon excitation experiment: transitions were observed with the $5d\,6p\ ^1F_3^o$ collisionally populated from the $6s\,7s\ ^3S_1$. Eleven new additive terms $6sng$ were observed in this experiment, the greater part of them in the vicinity of three new $5d\,7d$ $J = 4$ and 5 perturbers. For example, as it was shown in Table III, on both sides of the $5d\,7d\ ^3G_5$ (41 550 cm^{-1}), strong resonances were observed only with the $5d\,6p\ ^3F_4^o$ intermediate level and interpreted as $6s\,15g\ ^3G_5$ (41 539 cm^{-1}), $6s\,16g\ ^3G_5$ (41 603 cm^{-1}), and $6s\,17g\ ^3G_5$

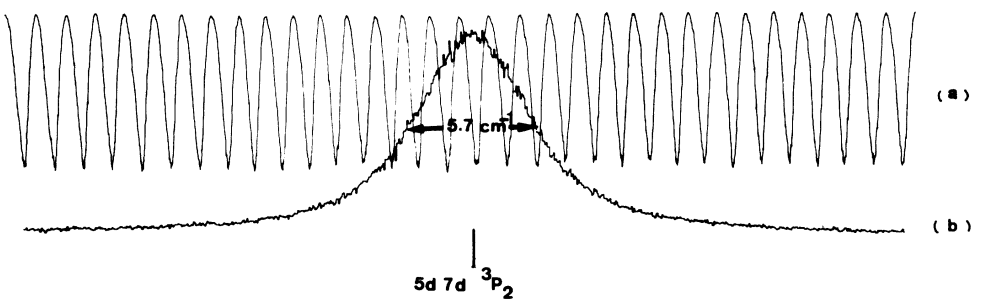

FIG. 7. Two-step optogalvanic spectrum of barium. (a) Fabry-Perot fringes $\Delta\sigma = 1.314\,67(8)$ cm^{-1}; (b) spectrum of Ba with $5d\,6s\ ^3D_2$-$5d\,6p\ ^3F_3^o$: 7280.3 Å for the first-step transition above the $6s$ ionization limit.

(41 653 cm^{-1}) states; the fine structure of the involved $6sng$ members is then partially resolved taking into account the $5d\,7d$ mixing effects. We observed identical phenomena near the $5d\,7d\ ^3G_4$ (40 974 cm^{-1}), $^3D_3$ (41 459 cm^{-1}), $^3F_3$ (41 726 cm^{-1}), and $^3F_4$ (41 845 cm^{-1}).

Figure 5 shows the two-step optogalvanic spectrum obtained from the $5d\,6p\ ^3F_3^o$ intermediate level. In the strong perturbed region between the $6s\,26d$ and $6s\,27d$ terms, three strong lines were identified to transitions with $5d\,7d$: $^3F_4$ and $^1D_2$, and $6s\,24g$: $J=4$. The bottom trace (c) is recorded without the first-step laser line showing the weak optogalvanic signal obtained with the dc. discharge population density of the atoms in the intermediate level. Intensity comparisons for the lines between traces (c) and (b) give evidence of a strong enhancement of the ionization signal in the two-step excitation process.

Figure 6 shows the end of the unresolved $6snd$ $J=2$, 3, and $6sng$ $J=3,4$ series below the $6s$ limit.

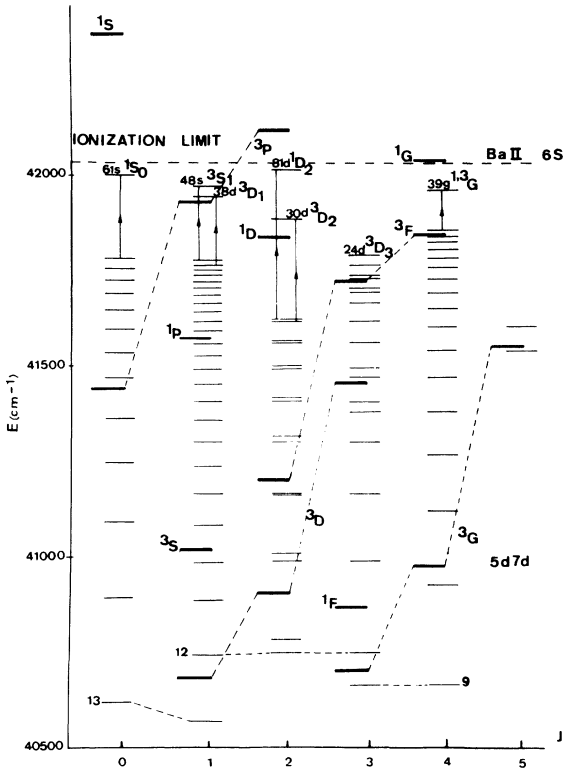

FIG. 8. Grotrian diagram of the even levels of Ba I above 40 500 cm^{-1}.

D. Observed $5d\,7d$ levels just above the first $6s$ ionization limit

Three missing levels of $5d\,7d$ configuration were found just above the $6s$ limit in the autoionizing region and then energy values are given in Table IV. Figure 7 shows the broad profile of the $5d\,6p\ ^3F_3^o - 5d\,7d\ ^3P_2$ transition. Extensive data have been recorded up to the $5d$ limits and will be published later.

IV. THEORETICAL ANALYSIS OF THE $5d\,6d$ AND $5d\,7d$ EVEN CONFIGURATIONS

Finally from these optogalvanic spectra 15 $5d\,7d$ new levels were observed and identified: 12 lay below the first ionization limit and 3 just above in the autoionizing region. The complete energy structure of $5d\,7d$ is shown on the Grotrian diagram reported in Fig. 8 using the LS-coupling scheme.

Theoretical energy of two $5d\,7d$ $J=2$ levels were initially predicted to $40\,886 \pm 75$ cm^{-1} for the $^3D_2$ state and $42\,100 \pm 50$ cm^{-1} for $^3P_2$ by Aymar and Robaux[8] from the MQDT analysis of the bound even-parity $J=2$ two-photon spectrum.[7] We ob-

TABLE V. Fitted fine structure parameters for the configurations $5d\,6d$ and $5d\,7d$ of Ba I.

Parameters	Values (cm^{-1})	
	$5d\,6d$	$5d\,7d$
E_0	37 145.3 ±5.2	41 478.6 ±2.6
$F_2(5dnd)$	32.9 ±0.8	13.9 ±0.4
$F_4(5dnd)$	1.07±0.22	0.48±0.12
$G_0(5dnd)$	741.6 ±6.3	306.1 ±3.3
$G_2(5dnd)$	11.4 ±0.7	3.8 ±0.5
$G_4(5dnd)$	1.01±0.20	0.38±0.09
Zeta $5d$	297.3 ±8.7	303.0 ±2.4
Zeta nd	37.0 ±10.1	22.8 ±2.8
	18 levels	18 levels
	$\langle \overline{\Delta E} \rangle = 17$ cm^{-1}	$\langle \overline{\Delta E} \rangle = 9$ cm^{-1}

served them, respectively, at 40 905 cm^{-1} and 42 118 cm^{-1} in very close agreement with MQDT predicted values.

However, to give a theoretical analysis of the other $5d\,7d$-observed levels, comparisons between experimental and calculated energies have been made using Racah's method[14] based on the Slater-Condon theory.[15,16] Fitted parameters on the whole $5d\,7d$ configuration are given in the second column of Table V. The root-mean-square error is 9 cm^{-1} representing 0.5% of the total energy range of the levels. Comparison between the energy observed (E_0) and calculated (E_c) are given in Table VI. Leading component of the eigenvectors are given in the LS- and $5d_{j1}7d_{j2}$-coupling schemes. As it was expected the level designation is closer to the

TABLE VI. Energy levels of $5d\,7d$ in Ba I.

J	E_C (cm^{-1})	E_0 (cm^{-1})	ΔE (cm^{-1})	Designation leading comp. % LS	jj
0	41 444.6	41 441.2	−3.4	$(75.2)^3P_0$	(97.3) 3/2 3/2
	42 368.9	42 370.5	1.6	$(75.2)^1S_0$	(97.3) 5/2 5/2
1	40 694.7	40 684.4	−10.3	$(68.5)^3D_1$	(97.4) 3/2 3/2
	41 023.2	41 019.5	−3.6	$(50.0)^3S_1$	(86.0) 3/2 5/2
	41 575.0	41 570.3	−4.7	$(54.0)^1P_1$	(98.7) 5/2 5/2
	41 924.2	41 930.9	6.7	$(80.7)^3P_1$	(88.7) 5/2 3/2
2	40 903.9	40 905.7	1.8	$(81.9)^3D_2$	(87.1) 3/2 5/2
	41 188.8	41 204.7	15.9	$(70.6)^3F_2$	(98.3) 3/2 3/2
	41 840.8	41 841.7	0.8	$(36.4)^1D_2$	(84.3) 5/2 3/2
	42 120.9	42 118.4	−2.5	$(59.6)^3P_2$	(97.1) 5/2 5/2
3	40 695.4	40 698.6	3.2	$(65.7)^3G_3$	(95.9) 3/2 3/2
	40 875.9	40 867.3	−8.6	$(28.7)^1F_3$	(87.1) 3/2 5/2
	41 454.3	41 459.3	5.0	$(63.2)^3D_3$	(99.8) 5/2 5/2
	41 733.9	41 726.6	−7.3	$(79.1)^3F_3$	(90.5) 5/2 3/2
4	40 968.7	40 974.3	5.5	$(82.1)^3G_4$	(88.1) 3/2 5/2
	41 850.9	41 845.6	−5.3	$(58.7)^3F_4$	(70.7) 5/2 3/2
	42 047.9	42 041.7	−6.2	$(60.9)^1G_4$	(79.0) 5/2 5/2
5	41 538.7	41 550.2	11.5	$(100)^3G_5$	(100) 5/2 5/2

TABLE VII. Energy levels of $5d\,6d$ in Ba I.

J	E_C (cm^{-1})	E_0 (cm^{-1})	ΔE (cm^{-1})	Designation leading comp. % LS	jj
0	37 697.9	37 675.8	−22.0	$(87.3)^3P_0$	(90.1) 3/2 3/2
	38 925.8	38 923.9	−1.9	$(87.3)^1S_0$	(90.1) 5/2 5/2
1	35 914.3	35 933.8	19.5	$(76.0)^3D_1$	(94.4) 3/2 3/2
	36 445.5	36 446.6	1.1	$(48.4)^3S_1$	(63.6) 3/2 5/2
	36 921.1	36 902.5	−18.6	$(46.5)^1P_1$	(95.0) 5/2 5/2
	38 009.5	38 023.2	13.7	$(95.3)^3P_1$	(70.9) 5/2 3/2
2	36 188.7	36 200.4	11.7	$(95.6)^3D_2$	(70.2) 3/2 5/2
	37 088.8	37 088.8	0.0	$(84.3)^3F_2$	(94.8) 3/2 3/2
	37 827.3	37 837.4	10.1	$(58.2)^1D_2$	(60.7) 5/2 3/2
	38 266.7	38 267.7	0.9	$(71.4)^3P_2$	(91.6) 5/2 5/2
3	35 911.3	35 894.3	−17.1	$(50.4)^3G_3$	(88.0) 3/2 3/2
	36 173.1	36 165.3	−7.8	$(45.1)^3G_3$	(65.6) 3/2 5/2
	36 644.1	36 628.9	−15.2	$(68.1)^3D_3$	(99.2) 5/2 5/2
	37 513.2	37 504.0	−9.1	$(93.9)^3F_3$	(73.9) 5/2 3/2
4	36 336.0	36 348.9	13.0	$(95.5)^3G_4$	(70.6) 3/2 5/2
	37 734.4	37 732.2	−2.1	$(86.9)^3F_4$	(47.8) 5/2 5/2
	38 166.6	38 177.1	10.5	$(86.7)^1G_4$	(52.1) 5/2 5/2
5	36 824.1	36 837.5	13.4	$(100)^3G_5$	(100) 5/2 5/2

jj coupling than the LS one: average value of the leading components are, respectively, 91.3 and 66.1%. Nevertheless, convenient LS designation is used in our energy level tables to facilitate identification with previous works.

Matrix elements being the same for $5dnd$ configurations with different n value, we have made the same study for the $5d\,6d$ low configuration. Fitted parameters are given in the first column of Table V and the rms error is 17 cm^{-1} representing also 0.5% of the level energy splitting. Comparison between the two sets of fitted parameter values for $5d\,6d$ and $5d\,7d$ configurations is consistant with general laws of variation in the central field approximation. Zeta $5d$ spin-orbit parameter is practically the same in both studies and zeta $6d$ and zeta $7d$ values follow the $1/n^3$ decrease expected for the spin-orbit radial integral of a $n\,l$ ($l \neq 0$) Rydberg electron. Calculated and observed energies for $5d\,6d$ levels are given in Table VII. Average values of the leading component are, respectively, 76.5 and 78.8 % in LS and jj schemes giving here only a small advantage to the second one. This parameter energy study removes definitely the ambiguity in the interpretation of the 38 923 cm^{-1} $J=0$ level given in the literature. This level has been successively identified to $6s\ 10s\ ^1S_0$ (Ref. 5) and $6p^2\ ^1S_0$ (Ref. 9) by general comparison of MQDT parameters for the Ca, Sr, and Ba sequences. Our calculation improved the $5d\,6d\ ^1S_0$ designation obtained by Aymar *et al.*[7] in their four-channel MQDT parametrization. $6p^2\ ^1S_0$ level is then unknown and should be searched elsewhere. Predicted energy from semiempirical calculations using strong interaction parameters R^1 $(5d^2, 6p^2)$ and R^3 $(5d^2, 6p^2)$ between $5d^2$ and $6p^2$ configurations is given by Wyart[17] at $44\,760 \pm 500$ cm^{-1}, i.e., above the $6s$ ionization limit. Further investigations from the $5d\,6p\ ^1P_1^o$ as intermediate level were undertaken.

V. CONCLUSION

In addition to the previous work on Ba using two-photon absorption spectroscopy and space-

charge detection of ions, we have performed a two-step laser excitation in a Ba discharge heat-pipe cell with an optogalvanic detection of the ions produced from the selectively excited states. This experiment, less restrictive in the J observed range values than the precedent one, has allowd us to extend the knowledge of the $J=1$, 3, 4, and 5 even levels of neutral barium from the low metastable $5d\,6s$ levels using $5d\,6p$ intermediate states. Complete level structure of $5d\,7d$ configuration is observed and interpreted in the semiempirical theory using Racah's method. The new levels of the $6sns$, $6snd$, and $6sng$ Rydberg series exhibit large mutual interaction with $5d\,7d$ levels and MQDT analysis of the $J=1$, 3, 4, and 5 spectra will be reported later. Extensive data in the autoionizing region between the $6s$ and $5d$ limits has been obtained and analysis of the spectra is in progress.

ACKNOWLEDGMENTS

We are grateful to Professor S. Feneuille for his stimulating interest and we thank D. Garces for giving us technical assistance in the different phases of the experimental work.

[1]P. Camus, M. Dieulin, and C. Morillon, J. Phys. Lett. 40, L513 (1979).
[2]F. M. Penning, Physica 8, 137 (1928).
[3]W. B. Bridges, J. Opt. Soc. Am. 68, 352 (1978).
[4]R. B. Green, R. A. Keller, P. K. Schenck, J. C. Travis, and G. G. Luther, Appl. Phys. Lett. 29, 727 (1976).
[5]D. J. Bradley, P. Ewart, J. V. Nicholas, and J. R. D. Shaw, J. Phys. B 6, 1594 (1973).
[6]J. R. Rubbmark, S. A. Borgström, and K. Bockasten, J. Phys. B 10, 412 (1977).
[7]M. Aymar, P. Camus, M. Dieulin, and C. Morillon, Phys. Rev. A 18, 2173 (1978).
[8]M. Aymar and O. Robaux, J. Phys. B 12, 531 (1979).
[9]J. A. Armstrong, J. J. Wynne, and P. Esherick, J. Opt. Soc. Am. 69, 211 (1979).
[10]P. Camus, J. Phys. B 7, 1154 (1974).
[11]G. Erez, S. Lavi, and E. Miron, IEEE J. Quantum Electron. 12, 1328 (1979).
[12]C. E. Moore, Atomic Energy Levels, Vol. 3, NBS Circular No. 467 (U. S. Government Printing Office, Washington, D. C., 1958) (unpublished).
[13]J. Verges (private communication, 1980).
[14]G. Racah, Phys. Rev. 61, 186 (1942).
[15]J. C. Slater, Phys. Rev. 34, 1293 (1929).
[16]E. U. Condon, Phys. Rev. 36, 1121 (1930); see also E. U. Condon and G. H. Shortley, *Theory of Atomic Spectra* (Cambridge University Press, Cambridge, 1935).
[17]J. F. Wyart (private communication, 1981).

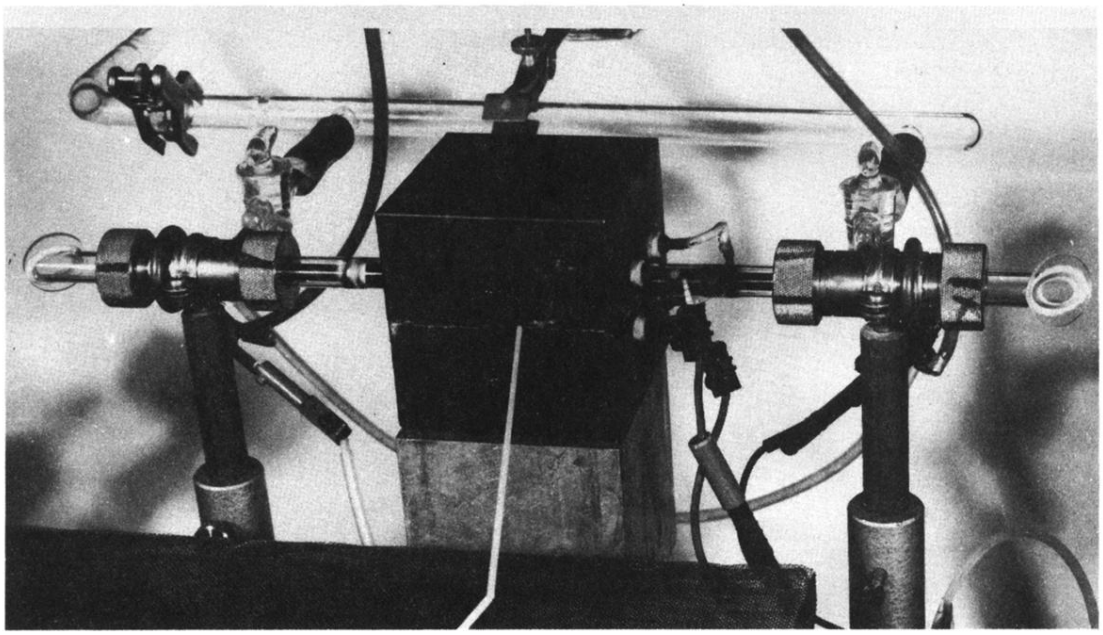

FIG. 2. Discharge heat-pipe cell for optogalvanic detection.